

# An investigation about the impact of the optimal reactive power dispatch solved by DE

Juan M. Ramirez<sup>a,\*</sup>, Juan M. Gonzalez<sup>b</sup>, Tapia O. Ruben<sup>c</sup>

<sup>a</sup> Cinvestav-Guadalajara, Av. Científica 1145, Col El Bajío, Zapopan, Jal. 45015, Mexico

<sup>b</sup> Universidad Tecnológica de Manzanillo, Manzanillo, Mexico

<sup>c</sup> Universidad Politécnica de Tulancingo, Hidalgo, Mexico

## ARTICLE INFO

### Article history:

Received 7 October 2009

Received in revised form 18 June 2010

Accepted 13 August 2010

### Keywords:

Optimization

Power system operation

Reactive power dispatch

Voltage stability

## ABSTRACT

With the advent of new technology based on power electronics, power systems may attain better voltage profile. This implies the proposition of careful strategies to dispatch reactive power in order to take advantage of all reactive sources, depending on size, location, and availability. This paper proposes an optimal reactive power dispatch strategy taking care of the steady state voltage stability implications. Two power systems of the open publications are studied. Power flow analysis has been carried out, which are the initial conditions for Transient Stability (TS), Small Disturbance (SD), and Continuation Power Flow (CPF) studies. Steady state voltage stability analysis is used to verify the impact of the optimization strategy. To demonstrate the proposal, PV curves, eigenvalue analyses, and time domain simulations, are utilized.

© 2010 Elsevier Ltd. All rights reserved.

## 1. Introduction

The problem of reactive power dispatch is generally bundled with the problem of maintaining load voltages within pre-specified limits. The generator voltage set-point values  $V_{Gi}^{ref}$  are optimized with respect to certain performance criteria subject to the reactive-power-balance constraints, the load voltage acceptable limits, the available limits on the generated reactive power, and the limits on voltage generators. The generation-based reactive power dispatch falls under the category of the optimal power flow (OPF).

Since transformer tap ratios and outputs of shunt capacitor/reactors have a discrete nature, while reactive power output generators, bus voltage magnitudes and angles are, on the other hand, continuous variables, the reactive power optimization problem is formulated as mixed-integer, nonlinear problem [1,2].

Algorithms based on the principles of natural evolution have been applied successfully to a set of numerical optimization problems. With a good degree of parallelism and stochastic characteristics, they are adequate for solving intricate optimization problems, such as those found in reactive optimization, distribution systems planning, expansion of transmission systems, and economic dispatch [3–9]. Publications present an extensive list of works concerning the application of evolutionary techniques to power systems issues [10,21,22]. In general, these applications concentrate

primarily on power system planning, followed by distribution systems.

Lai and Ma [3] have presented a modified evolutionary strategy to solve the reactive power dispatch, obtaining good results. Other authors [5,6] have applied the same algorithm for other power system problems, reporting results using the IEEE30 system. A simplified evolution strategy has been used in [6] and compared with genetic algorithms, and the Lai and Ma algorithm. More recently, a proposal quite similar to [3] has been presented in [7]. In spite of these efforts, evolutionary techniques have not yet explored completely power system applications [11].

Differential Evolution (DE) algorithm has been considered a novel evolutionary computation technique used for optimization problems. The DE and some other evolutionary techniques exhibit attractive characteristics such as its simplicity, easy implementation, and quick convergence. Generally speaking, all population-based optimization algorithms, no exception for DE, suffer from long computational times because of their evolutionary/stochastic nature. This crucial drawback sometimes limits their application to off-line problems with little or no real-time constraints.

In these kind of algorithms, within an  $n$ -dimensional search space, a fixed number of vectors are randomly initialized, and then new populations are evolved over time to explore the search space and locate the optima. Differential Evolutionary strategy (DE) uses a greedy and less stochastic approach in problem solving. DE combines simple arithmetical operators with the classical operators of recombination, mutation and selection to evolve from a randomly generated starting population to a final solution. The fundamental

\* Corresponding author. Tel.: +52 33 3777 3600.

E-mail addresses: [jramirez@gdl.cinvestav.mx](mailto:jramirez@gdl.cinvestav.mx) (J.M. Ramirez), [mgonzalez@gdl.cinvestav.mx](mailto:mgonzalez@gdl.cinvestav.mx) (J.M. Gonzalez), [rtapia@gdl.cinvestav.mx](mailto:rtapia@gdl.cinvestav.mx) (T.O. Ruben).

idea behind DE is a scheme whereby it generates the trial parameter vectors. In each step, the DE mutates vectors by adding weighted random vector differentials to them. If the fitness of the trial vector is better than that of the target, then the target vector is replaced by the trial vector in the next generation.

In this paper an optimal reactive power dispatch is proposed, where the objective function is the minimization of active power losses while maintaining system voltage security. In coordination with the problem formulation, Continuation Power Flow (CPF) is applied to evaluate and maintain the voltage security margin of the system. The control variables are the generation voltages, taps position, and capacitor/reactor banks. The problem is solved by the Differential Evolution algorithm. Usually, the problem is proposed as an objective function subject to constraints related to physical limits, especially on active and reactive power generation. Optimization techniques are applied to determine the steady-state optimal operating conditions, where voltage magnitudes and angles at all buses are evaluated for specific levels of load and generation. Evidently the results of any optimization technique will impact on the power system stability. In this paper the implication on steady state voltage stability is taken into account.

## 2. Optimal reactive power dispatch formulation

The optimal reactive power dispatch goal is to minimize active power losses and improve the voltage profile by setting generator bus voltages, VAR compensators, and transformer taps. This problem may be expressed as follows

$$\begin{aligned} \min f &= f_{\text{losses}} \\ \text{such that} \end{aligned}$$

$$\begin{aligned} P_i^d - P_i(V, \theta) &= 0 \quad i \in \text{NB} - 1 \\ Q_i^d - Q_i(V, \theta) &= 0 \quad i \in \text{NPQ} \end{aligned} \quad (1a)$$

$$\begin{aligned} V_{k\min} &\leq V_k \leq V_{k\max} \quad k = 1, 2, \dots, \text{NB} \\ \text{Tap}_{l\min} &\leq \text{Tap}_l \leq \text{Tap}_{l\max} \\ B_{\text{shunt},j\min} &\leq B_{\text{shunt},j} \leq B_{\text{shunt},j\max} \end{aligned} \quad (1b)$$

where  $f_{\text{losses}}$  represents the system losses; NB represent the system buses set; NPQ represents the PQ-buses set. Eq. (1a) represents the load flow equations.  $V$  is the bus voltage magnitude,  $\text{Tap}_l$  represents the  $l$ -th transformer's tap position, and  $B_{\text{shunt},j}$  is the shunt susceptance located at bus  $j$ . The generator bus voltages, the transformer tap-settings, and capacitor/reactor banks are the control variables.  $P_i^d - Q_i^d$  are the active and reactive power demand at bus  $i$ , respectively. In this paper, constraints (1a), (1b) are handled through the objective function's penalization, where the corresponding penalty parameters are chosen empirically based on experience and the particular application.

## 3. Summary on the Differential Evolution algorithm

Differential Evolution (DE) is a floating-point encoding evolutionary algorithm for global optimization over continuous spaces [12–14], which can work with discrete variables. DE creates new candidate solutions by combining the parent individual and several other individuals of the same population. A candidate replaces the parent only if it has better fitness value.

DE has three control parameters: amplification factor of the difference vector- $F$ , crossover control parameter-CR, and population size-NP. The original DE algorithm keeps fixed all three control parameters during the optimization process. However, there exists a lack on knowledge of how to find reasonably good values for the DE's control parameters for a given function [15].

Although the DE algorithm has been shown to be a simple, yet powerful, evolutionary algorithm for optimizing continuous functions, users are still faced with the problem of preliminary testing and hand-tuning of the evolutionary parameters prior to start up the actual optimization process. As a solution, self-adaptation has proved to be highly beneficial for automatically and dynamically adjusting evolutionary parameters, such as crossover and mutation rates. Self-adaptation is usually used in Evolution Strategies [16]. Self-adaptation enables an evolutionary strategy to adapt itself to any general class of problem, by reconfiguring itself accordingly, and does this without any user interaction.

### 3.1. DE's description

This subsection provides the basic background on the DE algorithm [14,17].

An optimization algorithm is concerned with finding a vector  $\mathbf{x}$  so as to minimize  $f(\mathbf{x})$ ;  $\mathbf{x} = (x_1, x_2, \dots, x_D)$ .  $D$  is the dimensionality of vector  $\mathbf{x}$ . The variables' domains are defined by their lower and upper bounds:  $x_{j,\text{low}}, x_{j,\text{upp}}$ ;  $j \in \{1, \dots, D\}$ . The initial population is selected uniform randomly between the lower ( $x_{j,\text{low}}$ ) and upper ( $x_{j,\text{upp}}$ ) bounds defined for each variable  $x_j$ . These bounds are specified by the user according to the problem's nature.

DE is a population-based algorithm and vector  $\mathbf{x}_{i,G}$ ;  $i = 1, 2, \dots$  NP is an individual in this population. NP denotes population size and  $G$  the generation. During one generation for each vector, DE employs mutation, crossover, and selection operations to produce a trial vector (offspring) and to select one of these vectors with the best fitness value.

Once initialized DE mutates randomly chosen vectors to produce an intermediary population of NP mutant vectors,  $\mathbf{v}$ . Each vector in the current population is then recombined with a mutant to produce a trial population of NP trial vectors. During recombination, trial vectors overwrite the mutant population, so that a single array can hold both populations.

### 3.2. Algorithm

The DE algorithm main steps are:

- Set the parameters:  $F$ , CR, NP, and the generation counter  $G = 1$ .
- Generate the initial population randomly:  $\mathbf{x}_{i,0}$   $i = 1, 2, \dots, \text{NP}$  from solution space.
- While (stopping criterion is not met).
- For each vector  $\mathbf{x}_{i,G} = \{x_{1i,G}, x_{2i,G}, \dots, x_{Di,G}\}$ ,  $i = 1, 2, \dots, \text{NP}$ .

(1) Choose three indexes  $r_1, r_2, r_3$  within the range  $[1, \text{NP}]$  randomly. They should be mutually different and also different from index  $i$ .

(2) (Mutation). Generate the mutant vector  $\mathbf{v}_{i,G+1}$  according to

$$\mathbf{v}_{i,G+1} = \mathbf{x}_{r_1,G} + F(\mathbf{x}_{r_2,G} - \mathbf{x}_{r_3,G}) \quad (2)$$

The scale factor,  $F \in (0, 1+)$ , is a positive real number that controls the rate at which the population evolves. While there is no upper limit on  $F$ , effective values are seldom greater than 1.0.

(3) (Crossover). DE crosses each vector with a mutant vector. Generate a new vector  $\mathbf{u}_{i,G+1}$ , where

$$\mathbf{u}_{i,G+1} = \begin{cases} \mathbf{v}_{i,G+1} & \text{if } r \text{ and } (j) \leq \text{CR} \text{ or } j = \text{rn}(i), \\ \mathbf{x}_{i,G} & \text{if } r \text{ and } (j) > \text{CR} \text{ and } j \neq \text{rn}(i), \end{cases} \quad (3)$$

$r(j) \in [0, 1]$  is the  $j$ th evaluation of the uniform random generator number.  $\text{rn}(i) \in (1, 2, \dots, D)$  is a randomly chosen index. The crossover probability, CR  $\in [0, 1]$ , is a user defined value that controls the fraction of parameter values that are copied from the mutant.



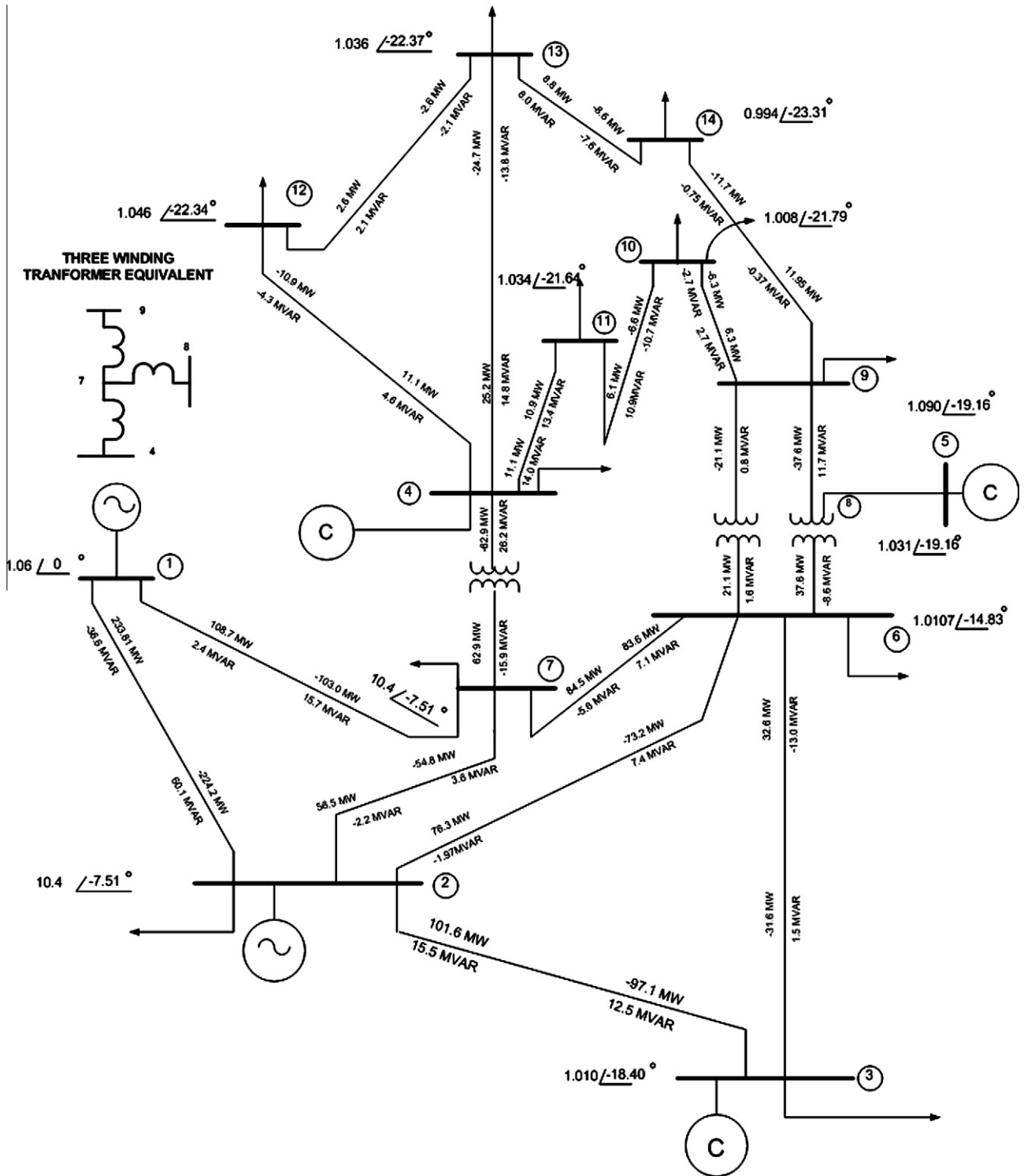


Fig. 2. Case 2: IEEE 14 bus test system.

voltages stemming from the optimization procedure try to keep a unitary magnitude, since de generators' magnitudes are kept within the interval [1.0, 1.05] p.u. This can be modified by allowing voltages' wider bounds.

Table 6 summarizes the active and reactive power generation, load, and losses at steady state. It is worth noting that the optimization procedure reduces the active and reactive power generation (especially the last one) as well as the system's losses.

#### 4.1.2. PV curves, eigenvalue analyses and time domain simulations

To verify the impact of the optimization results, it is important to verify the system's stability from the voltage stability point of view. Fig. 4 depicts the PV curve for the voltage magnitude at bus 5, under normal operating conditions and under contingencies on lines 5–4 and lines 5–7. As the load factor  $\lambda$  increases, the system approaches to an oscillatory instability, presenting a Saddle Node Bifurcation (SNB1) at  $\lambda = 2.567$ , while with lines 5–4 outage

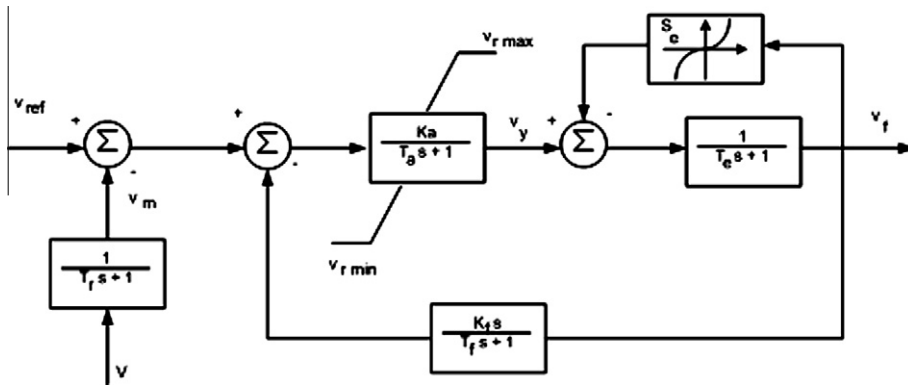


Fig. 3. Type II excitation system.

Table 2  
Generators' parameters.

Gen	$x_l$	$R$	$x_d$	$x'_d$	$x''_d$	$T'_{do}$	$T''_{do}$	$x_q$	$x'_q$	$x''_q$	$T'_{qo}$	$T''_{qo}$	$M$	$D$
1	0.0	0	0.146	0.0608	0	8.96	0	0.0969	0.0969	0	0.31	0	47.28	0
2	0.0	0	0.8958	0.1198	0	6	0	0.8645	0.1969	0	0.535	0	12.8	0
3	0.0	0	1.3125	0.1813	0	5.89	0	1.2578	0.25	0	0.6	0	6.02	0

Table 3  
Excitation systems' parameters.

Gen	$V_{rmax}$	$V_{rmin}$	$K_a$	$T_a$	$K_f$	$T_f$	NUSE	$T_e$	$T_r$	$A_e$	$B_e$
1	5	-5	20	0.2	0.063	0.35	0.01	0.314	0.001	0.0039	1.555
2	5	-5	20	0.2	0.063	0.35	0.01	0.314	0.001	0.0039	1.555
3	5	-5	20	0.2	0.063	0.35	0.01	0.314	0.001	0.0039	1.555

Table 4  
Steady state for the 9-buses power system.

Bus	$V$ p.u.	Ang deg	$P_g$ p.u.	$Q_g$ p.u.	$P_l$ p.u.	$Q_l$ p.u.
Bus 1	1.0000	0	0.7149	0.0241	0.0000	0.0000
Bus 2	1.0200	8.2493	1.6300	0.2896	0.0000	0.0000
Bus 3	1.0150	4.2378	0.8500	-0.1703	0.0000	0.0000
Bus 4	1.0218	-2.2589	0.0000	0.0000	0.0000	0.0000
Bus 5	1.0063	-4.0979	0.0000	0.0000	1.2500	0.4746
Bus 6	1.0148	-3.8094	0.0000	0.0000	0.9000	0.3000
Bus 7	1.0576	3.0850	0.0000	0.0000	0.0000	0.0000
Bus 8	1.0405	0.3117	0.0000	0.0000	1.0000	0.3500
Bus 9	1.0452	1.5973	0.0000	0.0000	0.0000	0.0000

Table 6  
Generation, load, and losses.

	Total generation	Total load	Total losses
<i>Base case</i>			
Real power (p.u.)	3.1964	3.15	0.04641
Reactive power (p.u.)	0.2284	1.1246	-0.8962
<i>OP case</i>			
Real power (p.u.)	3.1949	3.15	0.04489
Reactive power (p.u.)	0.14342	1.1246	-0.98118

Table 5  
Power flows for the 9-buses power system after optimization.

From	To	$S_{km}$ , p.u.
Bus 9	Bus 8	0.24472 - j0.09171
Bus 7	Bus 8	0.76058 + j0.09529
Bus 9	Bus 6	0.60528 - j0.11975
Bus 7	Bus 5	0.86942 + j0.04479
Bus 5	Bus 4	-0.4035 - j0.21936
Bus 6	Bus 4	-0.3080 - j0.09777
Bus 2	Bus 7	1.63000 + j0.28965
Bus 3	Bus 9	0.85000 - j0.17030
Bus 1	Bus 4	0.71489 + j0.02408

the system presents a SNB2 at point  $\lambda = 1.243$ . Likewise,  $\lambda = 1.6885$  for outage of lines 5–7 (SNB3).

Additionally, taken into account the optimized case (OP), the corresponding PV curves are depicted in Fig. 5. It is worth noting

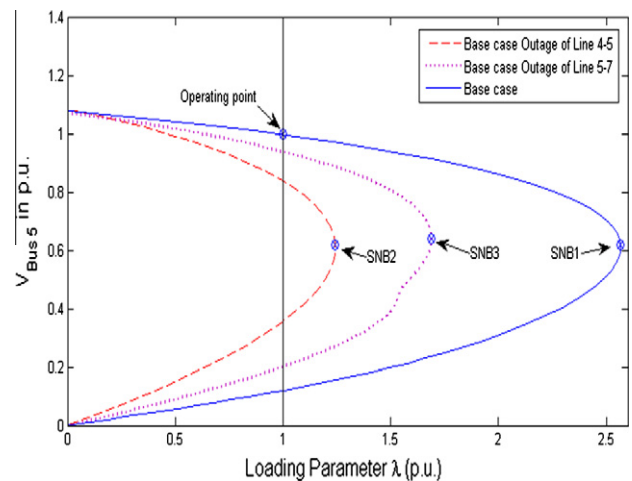


Fig. 4. PV curve for node 5.

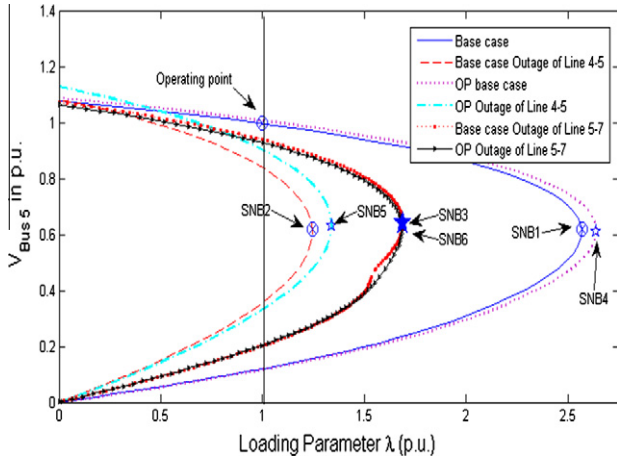


Fig. 5. PV curve for bus 5: base case and optimized one.

Table 7  
Critical mode, damping, and oscillating frequencies.

Case	Mode	Damping (%)	Frequency of oscillation Hz
	$\sigma \pm j\omega$	$\xi = -\frac{\sigma}{\sqrt{\sigma^2 + \omega^2}}$	$f = \omega/2\pi$
Base case outage lines 5–7	$-0.42778 + j1.3278$	0.3067	0.2113
OP outage lines 5–7	$-0.43295 + j1.3225$	0.3111	0.2105

that in these cases the optimization procedure increase the system's saddle node bifurcation (SNB4) at  $\lambda = 2.638$  and (SNB5)  $\lambda = 1.338$ . No significant modification is observed when lines 5–7 is out of service (SNB6).

Note from Fig. 5 that the operating point is close to SNB2–6 if lines 4–5 or lines 5–7 is out of service. Table 7 shows the eigenvalue closest to the operating point with lines 5–7 out of service, which is near to the positive axis. The optimization procedure in this case provide a damping even without changes observed on SNB (3&6), thus the system exhibits lower oscillations if the optimization is applied. This is demonstrated through time domain simulation, Fig. 6, which illustrates the angular velocities of generators when lines 5–7 is tripped and the optimization results are utilized. It can be seen that the system presents greater oscillation without optimization.

4.2. Case 2

The generators' and excitation systems' data are selected from [19] and are summarized in Tables 8 and 9, respectively.

4.2.1. Optimal power flow

The optimization technique is applied to the test system. Considering generation voltages, tap positions, and one shunt bank as susceptance in bus 14. The optimization gives rise to:  $V_{G1} = 1.050$  p.u.,  $V_{G2} = 1.040$  p.u.;  $V_{G3} = 1.000$  p.u.;  $V_{G4} = 1.050$ ;  $V_{G5} = 1.050$ ; Tap<sub>1</sub> = 0.950 p.u.; Tap<sub>2</sub> = 1.05 p.u.; Tap<sub>3</sub> = 0.9500 p.u.; Tap<sub>4</sub> = 1.050; Tap<sub>5</sub> = 0.950;  $B_{\text{shunt}} = 0.100$  p.u.

Notice that voltages obtained from the optimization technique keeps them close to 1 p.u. Bus voltages and power flow results are exhibited in Tables 10 and 11. These values are used in the Transient Stability (TS), Small Disturbance (SD), and Continuation Power Flow (CPF) studies.

Table 12 summarizes the active and reactive total generation, load and losses at steady state. There is an active power reduction in generation for about 1.27 MW, which is reflected on the active power losses, while a decrement in the reactive power for about 7.84 MVAR is achieved. Although the optimization technique improves the voltage profile, mainly due to the shunt capacitor

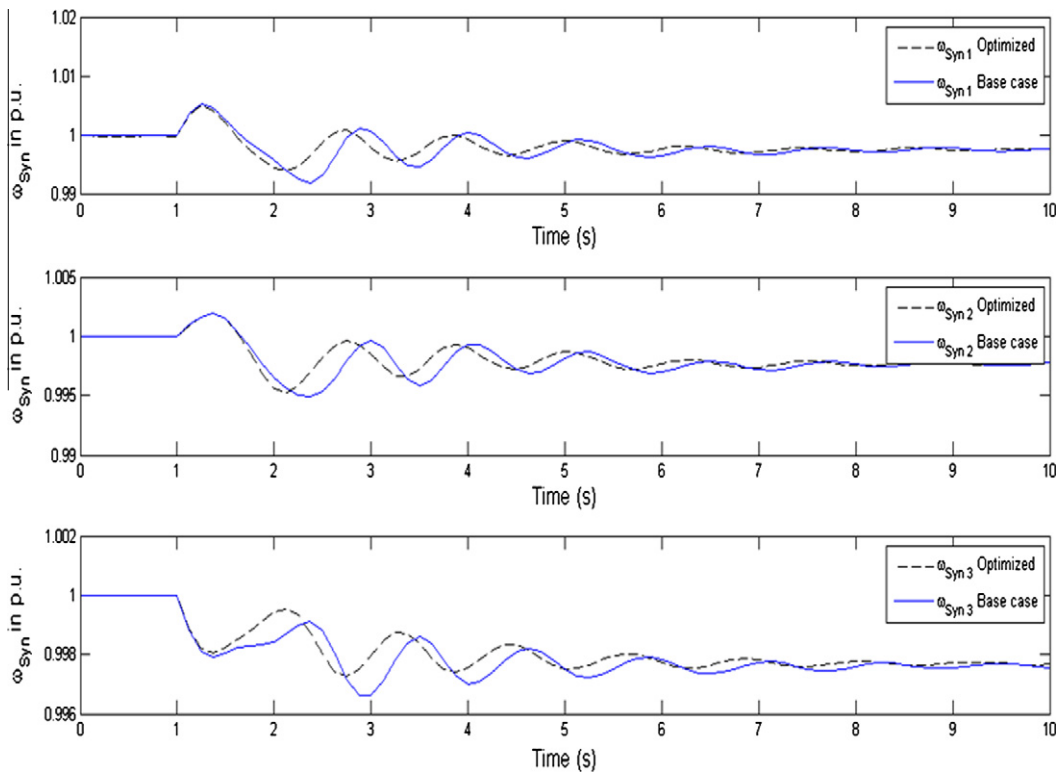


Fig. 6. Generators' speed after tripping lines 5–7.

**Table 8**  
Generators' data for Fig. 2.

Nod	$x_i$	$R$	$x_d$	$x'_d$	$x''_d$	$T'_{do}$	$T''_{do}$	$x_q$	$x'_q$	$x''_q$	$T'_{qo}$	$T''_{qo}$	$M$	$D$
1	0.2396	0.00	0.8979	0.6	0.23	7.4	0.03	0.646	0.646	0.4	0	0.033	10.296	47.28
3	0.0	0.0031	1.05	0.185	0.13	6.1	0.04	0.98	0.36	0.13	0.3	0.099	13.08	12.8
2	0.0	0.0031	1.05	0.185	0.13	6.1	0.04	0.98	0.36	0.13	0.3	0.099	13.08	6.02
8	0.134	0.0014	1.25	0.232	0.12	4.75	0.06	1.22	0.715	0.12	1.5	0.535	10.12	12.8
6	0.134	0.0014	1.25	0.232	0.12	4.75	0.06	1.22	0.715	0.12	1.5	0.21	10.12	6.02

**Table 9**  
Excitation systems' data for Fig. 2.

Gen	$V_{rmax}$	$V_{rmin}$	$K_a$	$T_a$	$K_f$	$T_f$	NUSE	$T_e$	$T_r$	$A_e$	$B_e$
1	7.32	0	200	0.02	0.002	1	0.01	0.2	0.001	0.0006	0.9
2	4.38	0	20	0.02	0.001	1	0.01	1.98	0.001	0.0006	0.9
3	4.38	0	20	0.02	0.001	1	0.01	1.98	0.001	0.0006	0.9
4	6.81	1.395	20	0.02	0.001	1	0.01	0.7	0.001	0.0006	0.9
5	6.81	1.395	20	0.02	0.001	1	0.01	0.7	0.001	0.0006	0.9

installed in bus 14 and the reduction in the generation of active and reactive power, there is a reactive power losses increment (2.64 MVAR) under this condition.

4.2.2. PV curves, eigenvalue analyses and time domain simulations

Two conditions are employed to evaluate the PV curves:

**Table 10**  
Steady state for the 14-buses system after optimization.

Bus	V p.u.	Ang deg.	Pg p.u.	Qg p.u.	Pl p.u.	Ql p.u.
Bus 1	1.0500	0	3.2649	-0.4503	0.0000	0.0000
Bus 2	1.0400	-7.2603	0.5480	0.7414	0.2973	0.1740
Bus 3	1.0000	-18.2332	0.0000	0.4188	1.2905	0.2603
Bus 4	1.0500	-21.0341	0.0000	0.5996	0.1534	0.1028
Bus 5	1.0500	-19.6228	0.0000	0.5826	0.0000	0.0000
Bus 6	1.0107	-14.8489	0.0000	0.5881	0.6549	0.0548
Bus 7	1.0202	-12.7732	0.0000	0.0000	0.1041	0.0219
Bus 8	1.0124	-19.6228	0.0000	0.5782	0.0000	0.0000
Bus 9	1.0380	-21.8332	0.0000	0.0000	0.4042	0.2274
Bus 10	1.0297	-22.1023	0.0000	0.0000	0.1233	0.0795
Bus 11	1.0350	-21.7574	0.0000	0.0000	0.0480	0.0247
Bus 12	1.0317	-22.2668	0.0000	0.0000	0.0836	0.0219
Bus 13	1.0274	-22.4518	0.0000	0.0000	0.1850	0.0795
Bus 14	1.0237	-23.9293	0.0000	0.0000	0.2041	-0.0363

**Table 11**  
Power flows for the 14-buses system after optimization.

From	To	$S_{km}$ p.u.
Bus 2	Bus 7	0.57284 - 0.05917i
Bus 4	Bus 12	0.10365 + 0.02609i
Bus 12	Bus 13	0.0188 + 0.00152i
Bus 4	Bus 13	0.23734 + 0.0639i
Bus 4	Bus 11	0.08718 + 0.03813i
Bus 11	Bus 10	0.03845 + 0.01183i
Bus 9	Bus 10	0.08533 + 0.06886i
Bus 9	Bus 14	0.13976 - 0.00849i
Bus 14	Bus 13	-0.06669 + 0.02289i
Bus 8	Bus 9	0.38781 + 0.27613i
Bus 1	Bus 2	2.2026 - 0.42511i
Bus 3	Bus 2	-0.97043 + 0.10243i
Bus 3	Bus 6	-0.32011 + 0.05603i
Bus 1	Bus 7	1.0623 - 0.02517i
Bus 7	Bus 6	0.87674 - 0.03848i
Bus 2	Bus 6	0.77706 - 0.05112i
Bus 7	Bus 4	0.58161 - 0.26029i
Bus 6	Bus 9	0.24142 + 0.06429i
Bus 6	Bus 8	0.38781 - 0.21334i
Bus 5	Bus 8	0 + 0.5826i

**Table 12**  
Generation, load, and losses for the 14-buses system.

	Total generation	Total load	Total losses
<i>Base case</i>			
Real power (p.u.)	3.8256	3.5483	0.27734
Reactive power (p.u.)	1.9705	1.1152	0.85536
<i>OP case</i>			
Real power (p.u.)	3.8129	3.5483	0.26463
Reactive power (p.u.)	1.8921	1.1152	0.88172

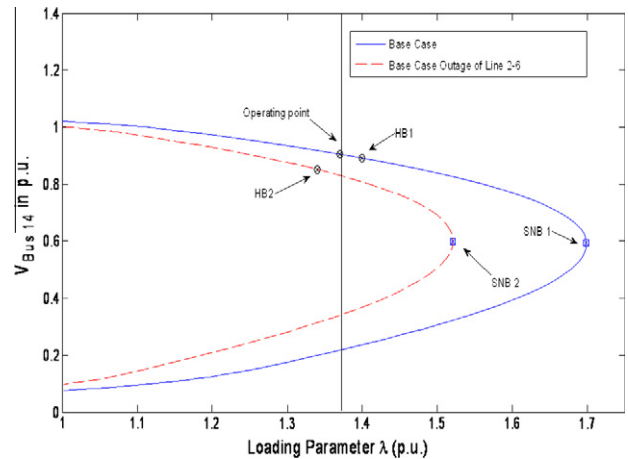


Fig. 7. PV curve for bus 14.

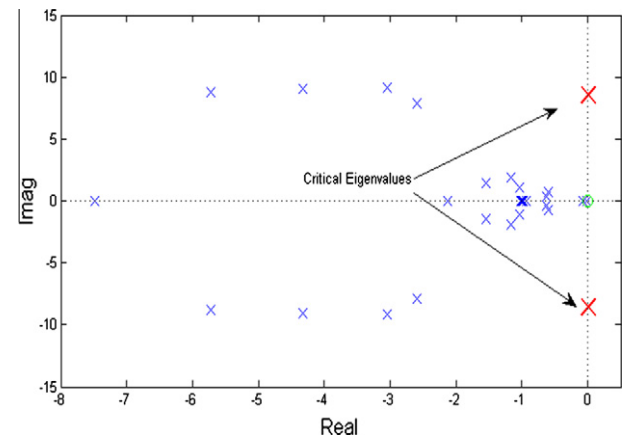


Fig. 8. Corresponding eigenvalues.

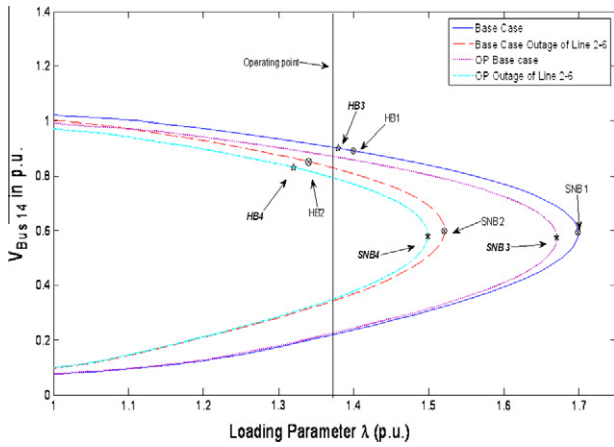


Fig. 9. PV curve of bus 14.

Table 13

Critical mode, damping, and oscillating frequencies.

Case	Mode	Damping (%)	Frequency of oscillation (Hz)
	$\sigma \pm j\omega$	$\zeta = -\frac{\sigma}{\sqrt{\sigma^2 + \omega^2}}$	$f = \omega/2\pi$
Base case outage lines 2–6	$0.07711 \pm j8.5398$	–0.9	1.3592
OP outage lines 2–6	$0.11802 \pm j8.5871$	–1.37	1.3667

1. Base case
2. lines 2–6 out of service

For the above mentioned conditions, the PV curves are depicted in Fig. 7. In these curves, the Hopf bifurcation (HB) points are obtained through eigenvalue analysis. In Fig. 7, as the loading factor  $\lambda$  increases, the system gets closer to the HB points. In HB points,

the system’s critical eigenvalues cross the imaginary axis. It can be observed that the system becomes unstable if HB is reached at  $\lambda = 1.4$  or at  $\lambda = 1.34$  with the lines 2–6 out of service. Fig. 8 exhibits the system’s eigenvalues for  $\lambda = 1.34$ , which correspond to HB point for the lines 2–6 outage. Critical eigenvalues ( $0.00933 \pm j8.5647$ ) are related to the excitation system in generator 1.

In order to study the power system behavior, the loading parameter is selected at 37% ( $\lambda = 1.37$ ). This point is selected due to its closeness to the HB. It is important to verify the impact of the optimization on the power system’s stability.

The PV curves for both the base case and the optimized-base case are shown in Fig. 9. Notice that the optimization procedure reduces the system’s loadability, shown through points SNB 3 and SNB 4, respect to those obtained for the base case SNB 1 and SNB 2, respectively, (SNB2 and SNB 3 correspond to the case where the lines 2–6 is out of service). On the other hand, it can be observed that for HB points, the optimization impacts negatively on the system, decreasing HB in all cases, i. e. for the base case HB is at  $\lambda = 1.4$  (HB1). Once the optimization is accomplished, HB decrease at  $\lambda = 1.38$  (HB3). For the case when the lines 2–6 is tripped, HB appears at  $\lambda = 1.34$  (HB2) for the base case, whereas a decrement in  $\lambda$  is observed at  $\lambda = 1.32$  with the optimization. Therefore, the optimization impacts on the system’s stability [20], showing that with the optimization the system becomes unstable faster, this is confirmed through eigenvalue analyses. Table 13 illustrates the critical mode associated to the excitation system of generator 1 at the operating point, with lines 2–6 tripped, for the base and optimized cases. It is noteworthy that the real part of the critical mode is moved even more to the positive axis. Thus, for this power system the optimization provides a negative damping. This is also shown in Table 13 where the damping ratio changes from –0.9 to –1.37, hence impacting on the system’s stability with higher frequency of oscillation. Likewise, results may be corroborated through time domain simulation, Fig. 10, where the lines 2–6 tripping at  $t = 1$  s is simulated. The generator’s angular velocities of generators 1 and 3 are illustrated in Fig. 10 where the major impact is exhibited.

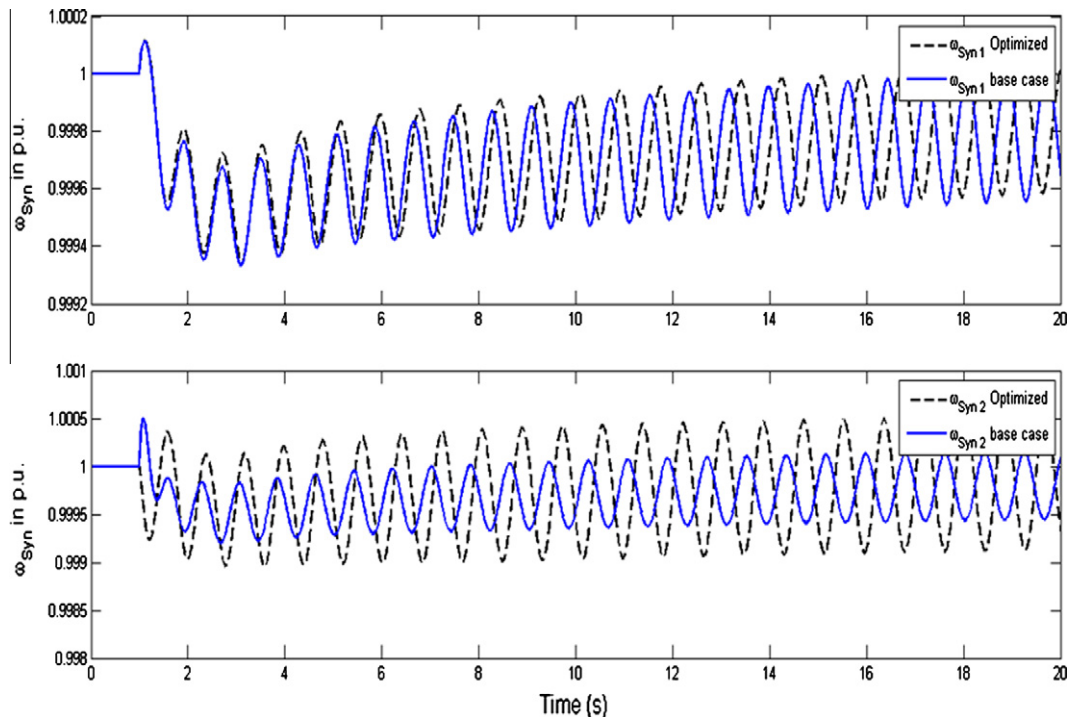


Fig. 10. Generators’ speed after the lines 2–6 tripping.

## 5. Conclusions

It is foreseen that the intelligent grid will require fast estimation indexes and measures available to the system's operators to assure operation within acceptable margins of reliability and security. In this paper, the authors emphasize that it is not enough to estimate an optimal solution. It is relevant that this solution assures appropriate conditions of security and reliability, so that additional studies are required. An optimal reactive power dispatch is proposed, where the objective function is the minimization of active power losses while maintaining system voltage security. In coordination with the problem formulation, Continuation Power Flow (CPF) is applied to evaluate and maintain the voltage security margin of the system.

An evolutionary computation technique was used to solve a reactive power dispatch formulated as the minimization of active power losses subjected to voltage constraints. The formulation was analyzed for two power systems controlling variables such as generation voltages, taps position, and shunt elements susceptances, showing a reduction not only on power system losses but also resulting in a power generation decrement. Results illustrate that in some cases even with losses' reduction, the impact on the stability is negative, since sometimes a reduction of SNB is presented and therefore the loadability of the system is reduced as well. Special care should be taken into account if the system presents HB and the operating point is close to HB or SNB, because if the optimization technique impact negatively, then the operating point could reach the HB or SNB point with the possibility of a voltage collapse.

In order to cope with this, it is important to take into account within the optimization procedure, mainly as a constraint, a voltage stability index which allows foresees a reduction in the dynamic performance before the optimization ends. A future paper will present such inclusion.

## Acknowledgment

The authors thank CFE-CONACyT under Grant 88160.

## References

- [1] Momoh James A, El-Hawary ME, Ramababu Adapa. A review of selected optimal power flow literature to 1993. Part I: nonlinear and quadratic programming approaches. *IEEE Trans Power Syst* 1999;14(1):96–104.
- [2] Varadarajan M, Swarup KS. Differential evolutionary algorithm for optimal reactive power dispatch. *Electr Power Energy Syst* 2008;30:435–41.
- [3] Ma JT, Lai LL. Optimal reactive power dispatch using evolutionary programming. *IEEE/KTH stockholm power technology conference*, Sweden; 1995. p. 662–7.
- [4] Yeh EC, Venkata SS, Sumic Z. Improved distribution system planning using computational evolution. *IEEE Trans Power Syst* 1996;11(2):668–74.
- [5] Lai LL, Ma JT. Application of evolutionary programming to reactive power planning – comparison with nonlinear programming approach. *IEEE Trans Power Syst* 1997;12(1):198–206.
- [6] Lee KY, Yang FF. Optimal reactive planning using evolutionary algorithms: a comparative study for evolutionary programming, evolutionary strategy, genetic algorithm and linear programming. *IEEE Trans Power Syst* 1998;13(1):101–8.
- [7] Park Y, Won J, Park J, Kim D. Generation expansion planning based on advanced evolutionary programming. *IEEE Trans Power Syst* 1999;14(1):299–305.
- [8] Manoharan PS, Kannan PS, Baskar S, Willjuice Iruthayarajan M. Evolutionary algorithm solution and KKT based optimality verification to multi-area economic dispatch. *Electr Power Energy Syst* 2009;31:365–73.
- [9] Baskar G, Mohan MR. Security constrained economic load dispatch using improved particle swarm optimization suitable for utility system. *Electr Power Energy Syst* 2008;30:609–13.
- [10] Lai LL. *Intelligent system applications in power engineering – evolutionary programming and neural networks*. John Wiley & Sons; 1998.
- [11] Gomes JR, Saavedra OR. Optimal reactive power dispatch using evolutionary computation: extended algorithms. *IEE Proc – Gener Transm Distrib* 1999;146(6).
- [12] Feoktistov V. *Differential evolution: in search of solutions*. New York: Springer; 2006.
- [13] Price KV, Storn RM, Lampinen JA. *Differential evolution. A practical approach to global optimization*. New York: Springer; 2005.
- [14] Storn R, Price K. Differential evolution—a simple and efficient heuristic for global optimization over continuous spaces. *J Global Optim* 1997;11:341–59.
- [15] Liu J, Lampinen J. A fuzzy adaptive differential evolution algorithm. *Soft Comput—Fusion Found Methodol Appl* 2005;9(6):448–62.
- [16] Bäck T. *Evolutionary algorithms in theory and practice. evolution strategies, evolutionary programming, genetic algorithms*. New York: Oxford University Press; 1996.
- [17] Rönkkönen J, Kukkonen S, Price KV. Real-parameter optimization with differential evolution. In: *The 2005 IEEE congress on evolutionary computation CEC2005*, vol 1. IEEE Press; September 2005. p. 506–13.
- [18] Anderson PM, Fouad AA. *Power system control and stability*. IEEE Press; 1994.
- [19] Milano F. *Power system analysis toolbox: documentation for PSAT version 2.0.0 beta*; March 2007.
- [20] del Valle Y, Venayagamoorthy G, Mohagheghi S, et al. Particle swarm optimization: basic concepts, variants and applications in power systems. *IEEE Trans Evol Comput* 2008;12(2):171–95.
- [21] AlRashidi MR, El-Hawary ME. A survey of particle swarm optimization applications in electric power systems. *IEEE Trans Evol Comput* 2009;13(4):913–8.
- [22] Xuexia Zhang, Weirong Chen, Chaohua Dai, et al. Dynamic multi-group self-adaptive differential evolution algorithm for reactive power optimization. *Int J Electr Power Energy Syst* 2010;32(5):351–7.
- [23] Mahadevan K, Kannan PS. Comprehensive learning particle swarm optimization for reactive power dispatch. *Appl Soft Comput* 2010;10(2):641–52.
- [24] Chaohua Dai, Weirong Chen, Yunfang Zhu, Xuexia Zhang. Reactive power dispatch considering voltage stability with seeker optimization algorithm. *Electr Power Syst Res* 2009;79(10):1462–71.
- [25] Abou El Elaa AA, Abidob MA, Spea SR. Optimal power flow using differential evolution algorithm. *Electr Power Syst Res* 2010;80(7):878–85.
- [26] He R, Taylor GA, Song YH. Multi-objective optimal reactive power flow including voltage security and demand profile classification. *Int J Electr Power Energy Syst* 2008;30(5):327–36.
- [27] Arya LD, Titare LS, Kothari DP. Improved particle swarm optimization applied to reactive power reserve maximization. *Int J Electr Power Energy Syst* 2010;32(5):368–74.